Nano Diesel Soot Particles Reduce Wear and Friction Performance Using an Oil Additive on a Laser Textured Surface

Jin-Fang Peng [1], Ming-Xue Shen [2],* and Zhen-Bing Cai [1],*

1   Tribology Research Institute, Traction Powder State Key Laboratory, Southwest Jiaotong University, Chengdu 610031, China; jinfangpeng3256@163.com
2   School of Materials Science and Engineering, East China Jiaotong University, Nanchang 330013, China
*   Correspondence: shenmingxue@126.com (M.-X.S.); czb-jiaoda@126.com or caizb@swjtu.edu.cn (Z.-B.C.)

Abstract: Tribological properties of nano diesel soot (DS) as an additive were investigated. Textures in linear radiating arrays were prepared on the surface of a spring-steel plate by laser radiation. The texture densities were 19.6%, 22.1%, and 44.2%, and the depth was 30 μm. The results indicated that the textured surface was interacted with additive favorably to improve its tribological performance. Friction coefficients and wear rates of textured surfaces with additive in oil were generally much lower compared to the original surface without additive. The higher area density of the textured surface with the additive in oil had the lowest friction coefficient, as low as 0.12, and also the minimum wear rate, as low as 1×10^3 μm/N·m in 100 °C, to be achievable. Such results can be attributed to the formation of the tribo-film and the storage function of the micro-dimple.

Keywords: oil additive; laser textured; anti-wear

1. Introduction

The exhaust from diesel engines contains a mixture of gases and very small particles that can create a health hazard [1] when not properly controlled. The diesel soot (DS) is usually regarded as a harmful substance, which is washed away in the exhaust system. Moreover, DS, which is generated from incomplete combustion of diesel oil, can flow into the friction interface, resulting in adverse effects. Researchers used grease, lubricating additives, machining operations, and ionic liquids to improve the friction and wear properties of mechanical parts. Hamilton et al. [2] established the concept of fabricating textured surfaces on mechanical components in 1966; since then, surface textures, such as micro-dimples or grooves, have been increasingly used to improve the tribological performance of friction pairs in engineering fields. Nakano et al. [3] investigated the tribological properties of cast iron and determined the effects of textured surfaces on the specimens. Textured surfaces were prepared by shot blasting or milling using a shaper. The friction coefficients of surfaces with groove and mesh patterns were higher than those of the original surfaces. Conversely, the friction coefficients of surfaces with dimpled patterns were lower than that of the original surfaces. These results indicated that the dimpled pattern had a beneficial effect on decreasing friction.

Zhang et al. [4] studied the tribological performance of sliding bearings in mixed or starved lubrication regimes. Square textures in linear radiating arrays were ablated on the surface of Babbitt alloy disks through laser radiation. Theoretical analysis demonstrated that proper texture arrangement generated a favorable distribution of micro-hydrodynamic pressure to significantly improve the tribological performance of the alloy. Yu et al. [5] discussed the average hydrodynamic pressure generated by texture patterns with circle, ellipse, and triangle dimples at different orientations relative to the sliding direction. The results indicated that ellipse dimples perpendicular to the sliding

direction showed the highest load carrying capacity. Li et al. [6] studied the preparation and tribological properties of graphene oxide/nitrile rubber nanocomposites under dry sliding and water-lubricated conditions and, finally, the friction and wear mechanisms of graphene oxide /nitrile-butadiene rubber (GO/NBR) nanocomposites were proposed. Etsion et al. [7–9] used the laser surface texturing (LST) technique to prepare different shapes of micro-dimples to improve the tribological performance of mechanical components. Braun et al. [10,11] studied the tribological behavior of steel with dimples ranging from 15 to 800 μm in diameter, and found the friction reduction of 80% was possible with the optimal diameter for certain sliding speeds. Gachot et al. [12–14] discussed the effects of surface textures under the operative lubrication regimes in the Stribeck curve, and summarized the fabrication methods and friction-reducing mechanisms. Researchers also conducted numerous studies to confirm that textured surfaces can enhance anti-wear performance [15,16]. The incompletely burned particles of diesel oil could scratch the surfaces of the mechanical components, possibly causing failure of the parts. These researchers found that the presence of DS is unfavorable for engine efficiency when soot accumulates to a certain amount. Hu et al. [17] investigated the morphology, structure, and composition of the biomass-oil soot particles. Hiralal et al. [18] used the DS as the oil additives, and compared the tribology behavior of the lubricating oil with different sizes and shapes of DS particles. Moreover, scholars studied several carbonaceous materials that can influence wear behavior [19–21]. Overall, we can conclude that texture can affect tribological performance and DS may cause severe wear.

In the present study, the characterization and particle size of DS was analyzed by high-resolution transmission electron microscopy (HR-TEM, JEM-2100F, JEOL, Tokyo, Japan) and atomic force microscopy (AFM, SPI3800N, Seiko Instruments Inc., Tokyo, Japan). A UTM-2 tribo-tester (CETR, Center for tribology, Campbell, CA, USA) was used to investigate the tribological properties of nano-DS particles as lubricant added to the textured surface.

2. Experiments

2.1. Materials

DS was removed and directly collected from the tailpipe of a four-cylinder diesel engine (from a large-scale passenger car exhaust pipe, Yuchai engine, eight years, Yulin, China). The structure of the DS is shown in Figure 1. Few nano-particles interacted with one other, leading to agglomeration (Figure 1a,b). The primary DS particle units appeared spherical or nearly spherical, with sizes ranging from 30 to 50 nm. The morphology of the DS surface was extremely irregular, and DS agglomerated to form a long chain (Figure 1a). AFM analysis was conducted to observe the nano-structure of DS (Figure 1c). More chemical characterization of the DS was analyzed in other works [22,23]. Lubricating oil (PAO4) was employed as the base oil, which was purchased from Sinopec Group (Beijing, China). PAO4 was always used as the lubricating oil, which had the best low- and high-temperature performance, and it could prolong the service life of the engine oil. The basic physicochemical properties of the samples are presented in Table 1.

Geometrical parameters and distribution should be first determined prior to fabrication. Laser fabrication presents advantages in terms of time-saving, low cost, and high efficiency. In this study, laser surface texturing was conducted on the 65Mn steel surface by using Nd:YAG pulse laser (wavelength of 1064 nm, laser frequency of 10 kHz, and pulse width of 5–25 ns). Different densities (19.6%, 22.1%, and 44.2%) of samples were designed to obtain the best area density. The geometries of the micro-dimple are summarized in Table 2. The concrete array and their geometrical texture parameters are illustrated in Figure 2. Figure 2a–c shows the SEM (manufacturer, city, country) images of the textured plates, respectively. Figure 2d,e reveal the 3D image and cross-section profiles of a single dimple, respectively. The edge of dimples were slightly higher than the height of the plate because of laser processing (Figure 2e). The high-energy action of the pulse laser resulted in ejection of the heated metal from the plate as well as partial deposition of the metal on the brim of the dimples. Prior to the wear test,

the surface was polished to remove asperity on the brims. The radius of the single dimple was 150 μm, and the depth was approximately 30 μm.
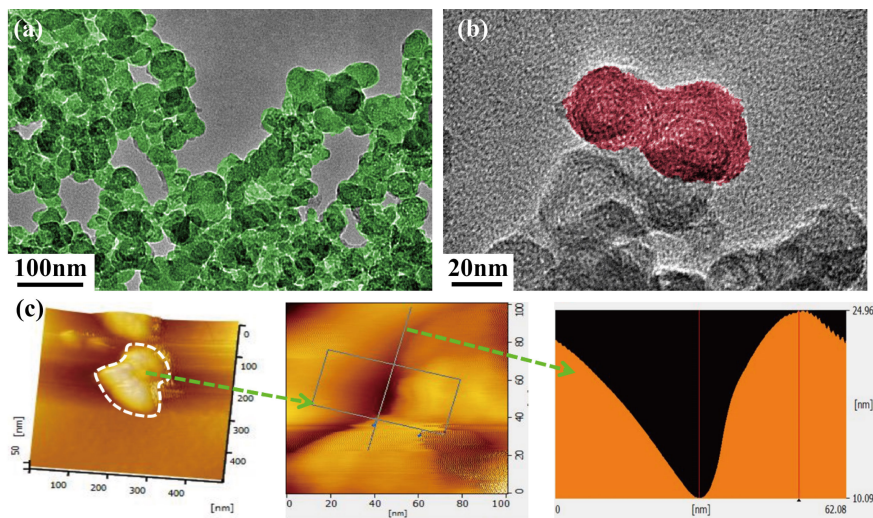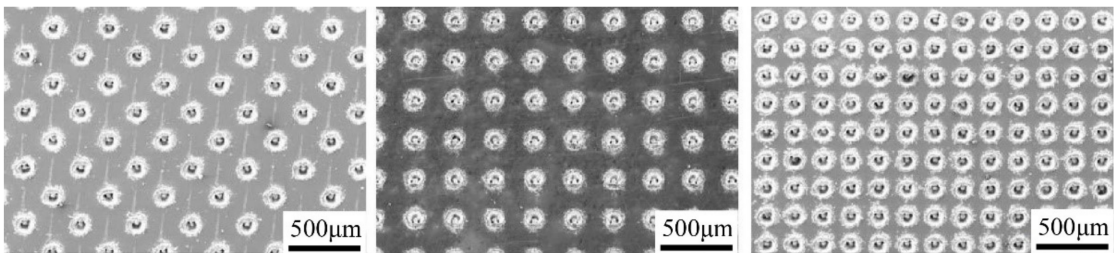

Figure 1. High-resolution transmission electron microscopy (HR-TEM) (**a**,**b**) and AFM images of diesel soot (**c**).

Table 1. Typical physicochemical properties of PAO4 oil.

Oil	Density (g·cm^{-3})	Kinematic Viscosity (mm^2·s^{-1})	Viscosity Index	Pour Point (°C)	Flash Point (°C)
PAO4	0.820	3.9, 100 °C/33.2, 25 °C	123	−73	270

Table 2. Parameters of the textured samples.

Item	0#	1#	2#	3#
Image	untextured			
Area density (%)	–	22.1	19.6	44.2
Distribution	–	Face centered	Square	Square
X–X distance (μm)	–	400	300	200
Y–Y distance (μm)	–	200	300	200
Depth (μm)	–	30	30	30

(**a**) 1# (α = 22.1%)　　(**b**) 2# (α = 19.6%)　　(**c**) 3# (α = 44.2%)
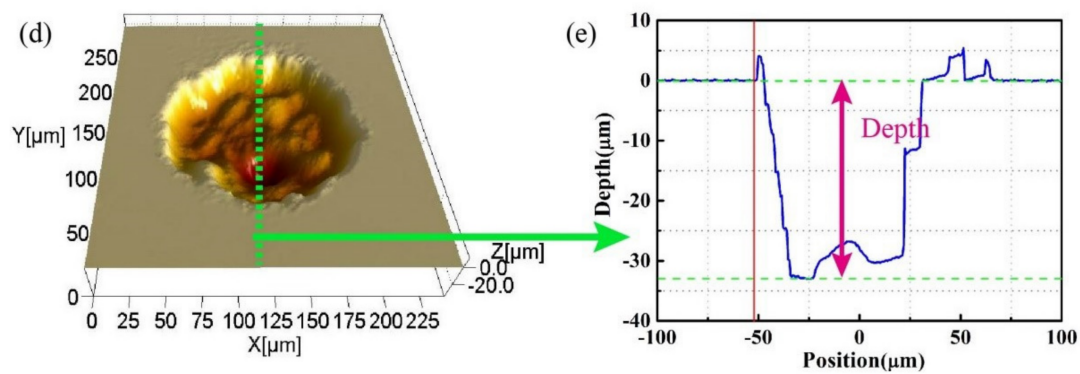
Figure 2. *Cont.*

Figure 2. Geometrical parameters and distribution of textured plates: (**a**–**c**) SEM images of the three different textured samples; (**d**) 3D image of a single dimple; and (**e**) cross-section profiles of a single dimple.

2.2. Test and Measuring Instruments

Friction and wear tests were conducted using GCr15 balls as the upper sample, with a diameter of 9.525 mm and hardness of 750 HV, as well as 65Mn plate as the lower sample, with dimensions of 25 mm × 14 mm × 6 mm and a hardness of 270 HV. The samples were purchased from Jinfu Mechanical and Electrical Center (Chengdu, China). The roughness of the balls was 0.4 μm, and the plate roughness was 1.5 μm. The entire wear process was performed on a UTM-2 tribo-tester under the following conditions: sliding speed of 5 mm/s, distance of 8 mm, normal load of 10 N, test time of 6000 s, and three temperature levels (room temperature of 25 ± 2 °C, 100 °C, and 175 °C). The lower plate sample was fixed in a square tank equipped with lubricating oil and remained stationary. The bottom of the tank was fitted with a heat device that can control and measure the experiment temperature. The illustration of the tribometer is shown in Figure 3. The specimens were cleaned with acetone and ethanol and then dried before each test. The tribological properties of the textured and untreated surfaces were tested under base oil (PAO4) and DS nanoparticles (0.01 wt %) well-dispersed in oil. To improve dispersibility, 1 wt % Span 80 ($C_{24}H_{44}O_6$, Chengdu Changzheng Glass Co., Ltd., Chengdu, China) was utilized as a dispersing agent. This results have been shown in other work [22,23]. The morphologies of the worn surfaces were analyzed through optical microscopy (OM, OLYMPUS BX50, Tokyo, Japan), SEM (JSM-7001F, JEOL, Tokyo, Japan), Raman spectrum (Lab Ram HR, Horiba Ltd., Kyoto, Japan) characterization, energy-dispersive X-ray spectroscopy (EDX, EDAX-7760/68M, Amptek, Bedford, MA, USA) and X-ray photoelectron spectrum (XPS, thermo-250Xi, Thermo Scientific, Waltham, MA, USA). The wear volume and wear rate are calculated by their 2D profile.
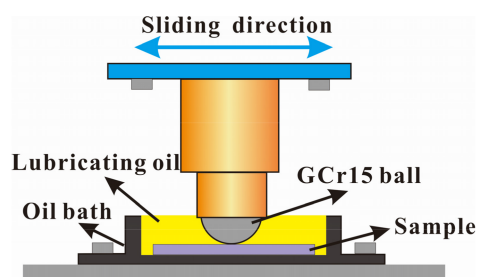

Figure 3. The illustration of the tribometer.

3. Results and Discussion

3.1. Friction and Wear Properties

Figure 4 shows various average friction coefficients at different temperature levels. At 25 °C, the average friction coefficients of all specimens were between 0.18 and 0.2. When the temperature was increased to 100 °C, all friction coefficients increased and followed the order of 2# (0.62) > 1# (0.61) > 0# (0.46) > 3# (0.31). The friction coefficients of the textured samples (2# and 1#) were higher than those of the original surface; conversely, the friction coefficient of 3# sample, which possessed high density, was lower than that of the original surface. In 100 °C, all samples presented a higher coefficient (COF) than at room temperature and 175 °C. This may be caused by adhesive wear. Due to the temperature increasing, the adhesive wear increased and COF increased. The tribological behavior of the textured surface depended on the test conditions. Hence, the textured surface of 2# and 3# increased the COF in 100 °C. With the temperature increasing, the viscosity decreased. The friction coefficient further decreased when the temperature increased to 175 °C. This phenomenon could be explained by two important factors, namely, viscosity change and friction oxidation. The contact interface would form a thinner oil film and the film separated the two tribo-pairs and reduced the friction. However, the thinner oil film aggravated wear and produced more debris. Hence, the COF firstly increased and then decreased with increasing temperature. On the other hand, the friction force was related to the number of micro-dimples. The friction coefficient decreased when sufficient micro-dimples were available to store the lubricating oil [2]. Of all the cases, 3# exhibited excellent tribological performance. The friction coefficients of the textured samples were irregular, but the cross-section profiles were regular and clear (Figure 5a–c). All textured samples presented shallower depths and smaller widths compared with those of the untreated samples, except the 2# textured surface at 100 °C. The anti-wear properties of the textured samples were better than those of the untreated samples, especially at high temperatures. For example, the wear rate of 3#, 2#, and 1# decreased to 77%, 73%, and 68%, respectively, compared with that of 0# (Figure 5d). With increasing temperature, the wear rate of each samples increased. With the increasing temperature, the viscosity decreased, and this will lead to a thinner oil film. Meanwhile, the wear debris was intense movement and formed a three-body layer in the tribology interface and increased the wear. The wear induced by the mechanical removal function at high temperature was strengthened and it caused more material loss and substantial wear debris. Overall, the textured surfaces may decrease friction resistance and the anti-wear performance was excellent at 25 °C and 175 °C, following the order of 3# > 2# > 1# > 0#.

To investigate the effect of DS as an oil additive on the textured surface, the friction coefficient curves of the untreated plate and three types of textured surfaces with DS as additive was compared (Figure 6). The friction coefficients of the 1# and 2# textured plates were relatively higher than those of the smooth plates, implying that surface texturing may result in higher friction force. When the base oil was used, the friction coefficient presented a high value and acute fluctuation. In addition, the friction coefficient exhibited low values and minimal fluctuation under lubricating oil containing 0.01 wt % DS. Since the adhesive wear in 100 °C is very severe, the fluctuation of COF in the untreated sample is the maximum. However, the contact interface of the textured surface is discontinuous, which leads to the fluctuation of the COF decrease. In general, the friction coefficients of samples lubricated by base oil with DS were considerably lower than that of samples lubricated by oil only. Since the DS would come to the friction interface, and the friction mode changed from sliding friction to rolling friction [24], the friction coefficient remained at a constant level of 0.12. An interesting phenomenon was observed on sample 3#. When the test time reached 3000 s, the friction coefficient decreased significantly. Since, in the higher-textured area density, more edges were in contact and so higher pressure build-up would occur. The contact interface would form a lubricating oil film, which separates the two tribo-pairs and reduces friction.

The effect of the textured surface on wear reduction is shown in Figure 7a. The results indicated that: (1) micro-dimples can reduce wear; and (2) the effect of micro-dimples in combination with

DS illustrated good tribological properties. Both friction coefficient and wear volume significantly decreased. The wear rate of plates lubricated by oil containing DS was lower than that of plates lubricated by the base oil. Figure 7b indicates that textured plates lubricated by the base oil containing DS exhibited a lower wear rate at each temperature. The additive played a significant role during the test, and the wear rate of the smooth plate lubricated by oil containing the additive reduced to a minimum of 92% at 175 °C compared with that lubricated by base oil. Regardless of the type of textured plates under lubrication, wear rates decreased considerably. Among the samples, 3# + DS possessed the optimal tribological performance. Textured surface was widely associated with possible mechanisms for improvement of tribological property; these mechanisms included (1) secondary lubrication, (2) collect wear debris, and (3) the micro-hydrodynamic effect. Overall, surface texture could reduce friction and wear, and the textured surface combined with the additive exerts the optimal effect under lubrication.
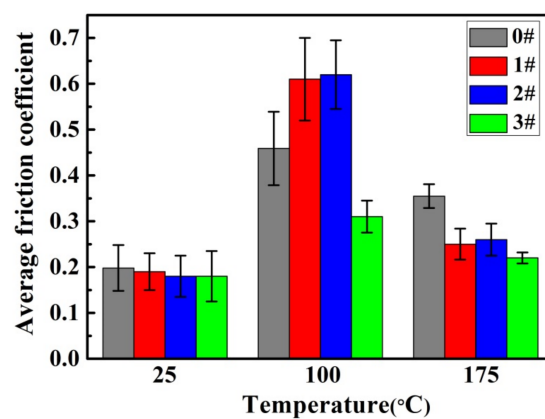

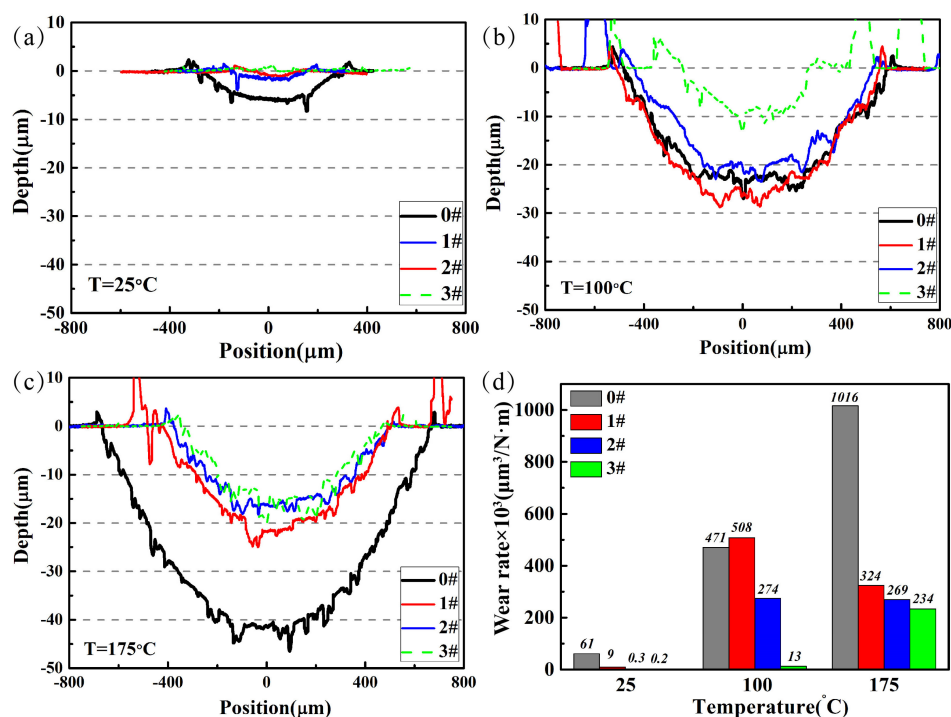**Figure 4.** Average friction coefficients of different samples.

Figure 5. Cross-section profiles of the worn plates at varied temperatures: (**a**) *T* = 25 °C; (**b**) *T* = 100 °C; (**c**) *T* = 175 °C; (**d**) wear rate of different samples at varied temperatures.

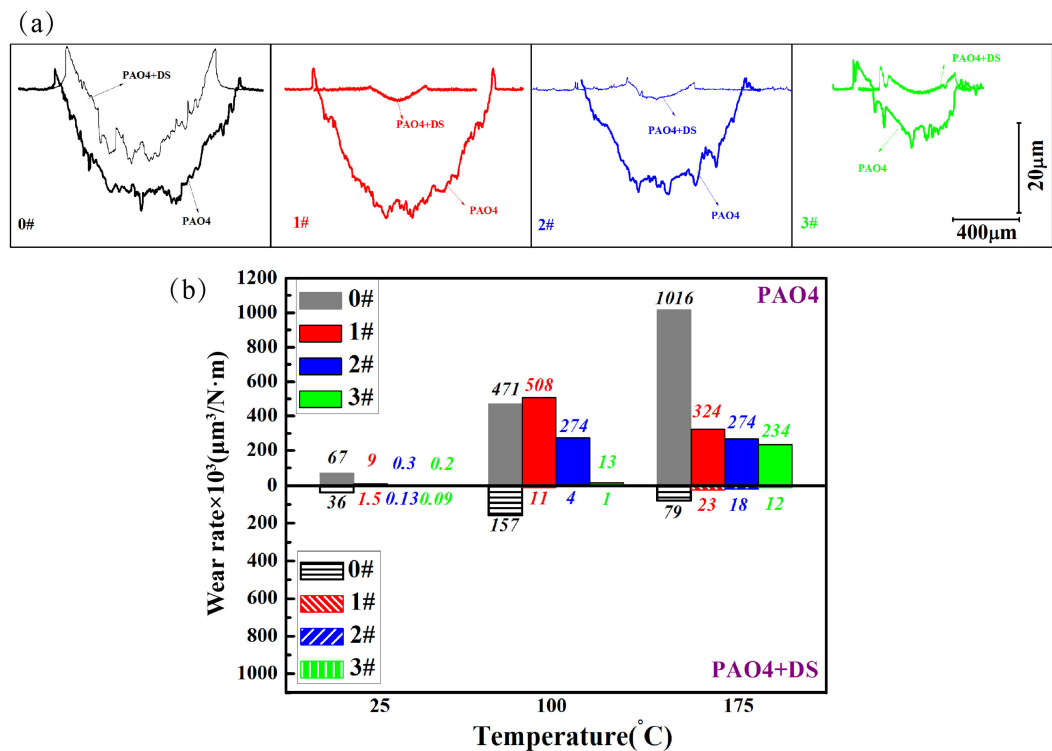**Figure 6.** Friction coefficient curves of different samples (*T* = 100 °C): (**a**) 0#; (**b**) 1#; (**c**) 2#; (**d**) 3#.

Figure 7. Cross-section profiles of worn plates at (**a**) *T* = 100 °C; (**b**) wear rates of different samples in different temperature.

3.2. Optical Microscopy and SEM Analysis of the Worn Surface

Optical microscopy images of the worn surface were obtained under the same conditions ($T = 100\ ^\circ\text{C}$) after friction tests. Figure 8 shows that the edge of the worn plate surface presented as multiple colors due to the formation of tribo-film on the worn surface. In addition, the microscopy image of the worn ball revealed that the micro-dimple caused a decrease in the actual contact area. Worn single dimples were observed on the worn ball surface, and the decreased contact area led to material loss.
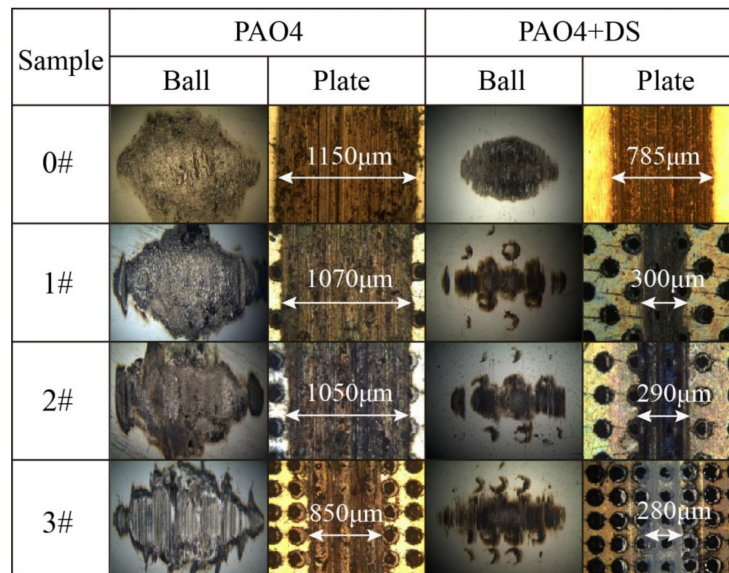

Figure 8. Optical microscopy of the worn surfaces ($T = 100\ ^\circ\text{C}$).

All the samples were cleaned with acetone prior to the SEM test. The smooth surface lubricated with pure PAO4 is shown in Figure 9a,b. Apparently, adhesive trace was observed on the surface and the material spall, which was the typical characteristics of abrasive wear. The result was in agreement with the cross-section profile in pure PAO4 (Figure 7), thereby confirmed that PAO4 provided minimal protection to the friction pair. The morphology of the 65Mn plate surface with DS as the additive differed from that of pure PAO4 (Figure 9c,d). Although obvious adhesive traces existed, the surface was smoother. DS nanoparticles possibly prevented the formation of tribo-film, and the anti-wear property could induce the functional DS. According to AFM and HR-TEM results, the DS additive could act as numerous small balls between the two contact surfaces to decrease friction and wear.

Figure 10 displays the SEM morphology of the worn surface in pure PAO4 and the combined function of the micro-dimple and additive. The discontinuity of the micro-dimple can promote the formation of the tribo-film and the storage function of the debris, thereby protecting the contact surface. Therefore, the textured plate lubricated by PAO4 exhibited better tribological properties than the smooth plate.

Notable results were observed that combined effect of dimples and additives. Figure 9c,d and Figure 10c,d shows dimples filled with DS additives during the sliding process. The single effect of textured surfaces or additives exhibited good anti-wear performance, whereas the combined effect showed excellent performance. Interestingly, in the case of PAO4 + DS, the depth and width decreased severely, and more residual dimples were detected on the worn surfaces (Figure 10c). Although the SEM images presented a higher amplification factor, the worn textured surface lubricated with oil containing the additive was considerably smoother, and the structure of residual dimples was completely protected. Sample 3# lubricated by oil containing the additive displayed the optimal tribological properties.
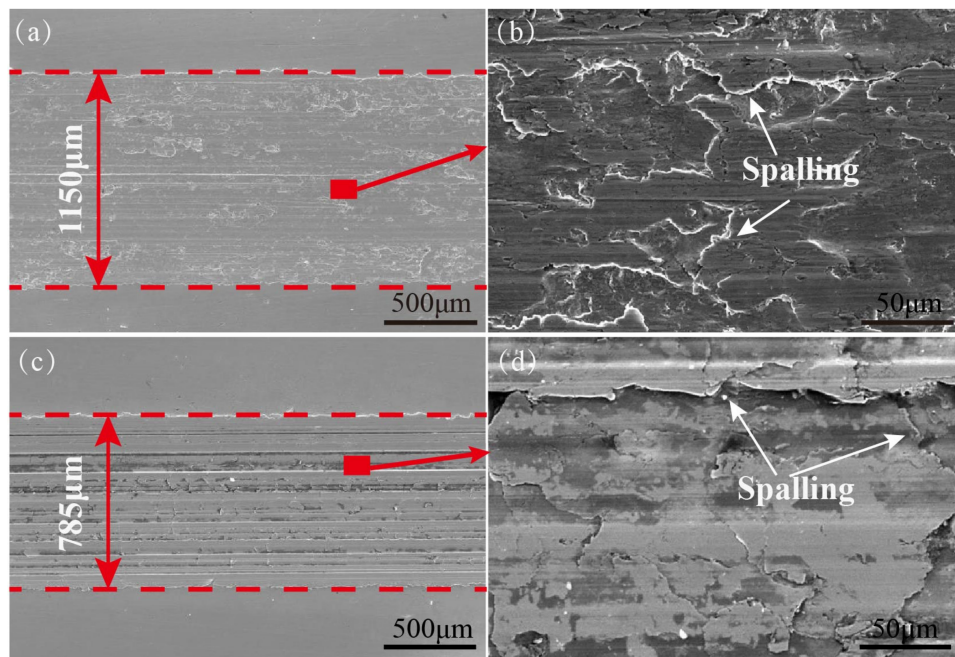
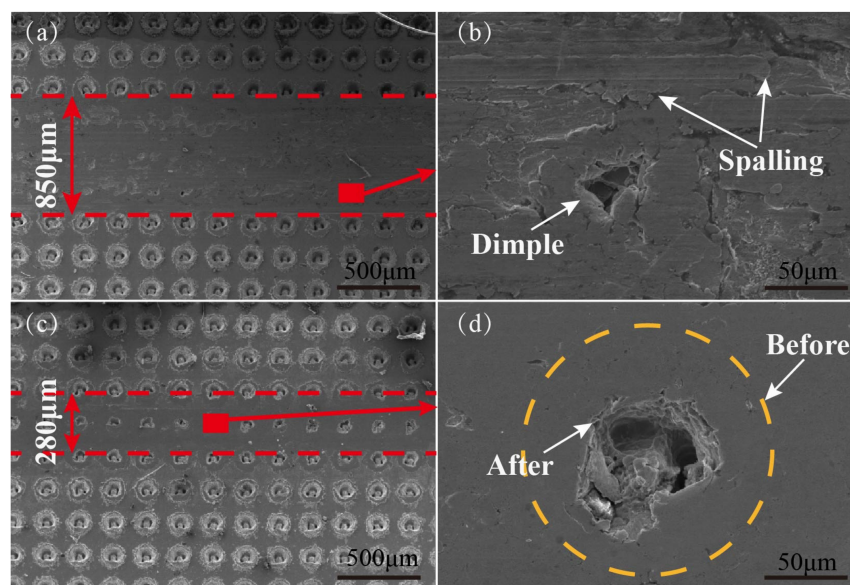**Figure 9.** SEM images of worn plates (0#, 100 °C): (**a**,**b**) PAO4; (**c**,**d**) PAO4 + DS.

Figure 10. SEM images of the worn plates (3#, 100 °C): (**a**,**b**) PAO4; and (**c**,**d**) PAO4 + DS.

3.3. Analysis of the Worn Surfaces

Figure 11 shows the analysis results of EDX spectra and elements content at three different locations: (1) the non-contact of the surface, (2) the worn dimple on the worn surface, (3) the worn surface lubricated by oil containing 0.01 wt % DS. Evidently, O appeared on the worn surface lubricated by the base oil with the additive, whereas only C and Fe were observed on the metallic matrix. In comparison with the non-contact, the lubricated regime may form a tribo-film on the worn surface, which contained Fe, O, C, and Mn [25]. Additinally, the detailed element contents are present in Table 3.
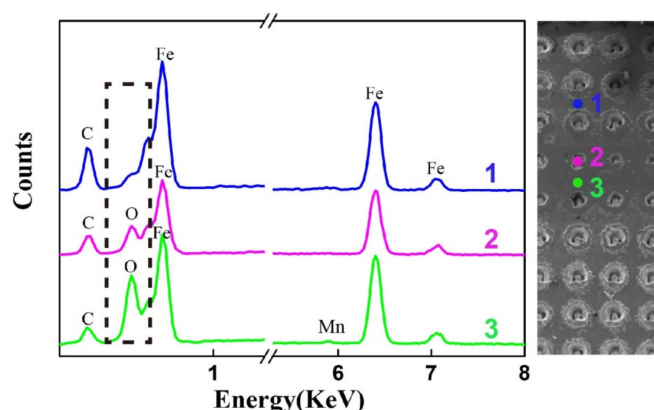
Figure 11. EDX spectra of different location from worn plate 3#: (**1**) the non-contact of the surface; (**2**) the worn dimple on the worn surface; and (**3**) the worn surface lubricated by the oil containing 0.01 wt % DS.

Table 3. Elemental content (at.%) corresponding to the EDX spectra in Figure 10.

Postions	C (%)	O (%)	Fe (%)
1	60.41	0	35.59
2	41.05	16.54	42.40
3	25.62	28.92	44.73

The XPS of textured worn plate lubricated by DS under 100 °C is shown in Figure 12. The O 1*s* peak is shown in Figure 12a, with a broad asymmetric spectrum that indicates various oxygen bonding environments. The O 1*s* peak was decomposed into two components, and the binding energies of 532.8 and 533.3 eV was attributed to C–O and H_2O, respectively. The XPS of C 1*s* peaks (Figure 12b) appearing at the bonding energies of 284.8 and 285.18 eV belonged to C–C/C–H and C, respectively.
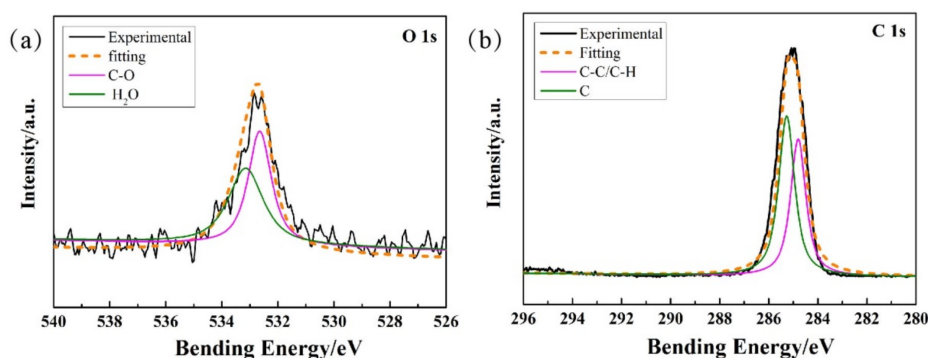

Figure 12. XPS of textured worn plate #3 lubricated by DS (*T* = 100 °C): (**a**) Oxygen element; (**b**) Carbon element.

The effect of additive combined with the textured surface is complicated. However, the single influence of the additive can be summarized as follows:

DS can act as numerous balls between the two contact surfaces (Figure 13a) [24]. The spherical structure of DS is destroyed during the sliding process, as can be proven by Raman spectra (Figure 13a). The two obvious peaks in the Raman spectra are the D and G peaks. The D peak at 1320 cm^{-1} was known as the disorder band, which corresponds to the sp^2 hybridized health defects. The G peak at 1580 cm^{-1} indicates the vibration in all of the sp^2-bonded carbon atoms, thereby denoting a "defect-free"

graphitic character. The ratio of D and G peak can be used to characterize the sp^3/sp^2 bonding ratio. The D peak with large width and higher ratio of D and G peak in worn plate than that of the original DS indicates that highly disordered and defect characteristics of the DS particles. The structure integrity break of DS is caused by shear force during the friction process. When the structure integrity breaks, the additives will absorb some of the energy. Thus, the friction pair lubricated by oil with DS exhibits better tribology performance in comparison with pure PAO4.

The single influence of texture can be summarized as follows:

The micro-dimple can storage oil and wear debris (Figure 14b) lead to friction reduction [26]. When the GCr15 ball is sliding, the lubricating oil stored in the micro-dimples can quickly add to the contact surface. Direct contact between surfaces can be prevented because of a steady supply of lubricating oil [27]. As is shown in Figure 13b, the Raman spectra exhibits several peaks at 615 and 664 cm^{-1}, which is the characteristic peak of Fe_2O_3 and Fe_3O_4, respectively. The existence of oxide reveals that the tribo-chemical reaction occurs at the contact interface. Oxidation wear is one of the wear mechanism. Therefore, the micro-dimple functions as storage during the test.

The influence of the additive in combination with the micro-dimple can be summarized as follows (Figure 14c):

The micro-dimples not only promote the formation of the oil film, but also stores DS particles and wear debris. We select three different positions to obtain Raman spectra: smooth surface, worn surface, and worn dimple. To compare the Raman spectra of different point, Gaussian fitting is applied for the D and G peaks fitting (Figure 15a–d). The fitting results of these two peaks' intensities and the intensity ratio of the D peak to G peak (I_D/I_G) are also shown in Figure 15e,f. As shown in Figure 15e,f, the intensity of the D and G peaks follows the order: 3 < DS < 1 < 2, and the I_D/I_G follows the order: DS < 1 < 3 < 2. As displayed in Figure 15f, the ratio of D and G peaks on the worn surface is considerably higher than those of the worn dimple, thereby indicated that the micro-dimple could protect the DS particles and the DS additives on the textured surfaces undergo more significant graphitization than that of original DS during friction, probably attributed to that the large amount of graphitized wear debris entrapped in the micro-dimples according to Ferrari and Robertson's three-stage model for the Raman spectra of disordered and amorphous carbon [28]. When the ball is sliding through the dimples, the additives in the dimples would be rolling or sliding in the dimples to decrease friction [29,30]. The ratio of D and G peaks in the smooth surface is similar to the original DS particles, which prove that the dimples could collect the unbroken additives. The higher ratio of D and G peaks in the worn surface also demonstrate that the structure integrity of DS is broken. The G peak of the worn surface is also higher than that of the worn dimple and smooth surface, which reveals that the detected substance is similar to graphite. These findings prove that the structure of the additive in contact surfaces change from spherical to graphite sheet. Since the spherical structure of the DS would access the contact surface and change the friction mode from sliding friction to rolling friction, the shear force would break the spherical structure of the DS and change the spherical structure to a graphite sheet during the friction process. Hence, the G peak of the worn surface is higher than that of original DS particle. The lubrication mechanism can be summarized. The original DS particle is regularly distributed in the PAO oil. During the test, the DS particle would access the contact interface and change the friction mode from sliding friction to rolling friction. Meanwhile, the dimple would store the DS particles and collect wear debris, which reduces friction and wear. As the test goes on, the shear force would break the spherical structure of DS and change the spherical structure to graphite sheet, and then lose lubrication. However, when the ball slid through the dimples, the DS particles stored in the dimple will release, which ensures that the DS particles with spherical structure perpetually occur at the contact interface and maintain the low-friction coefficient. As a result, the higher density of the textured surface with the additive in oil has the lowest friction coefficient.
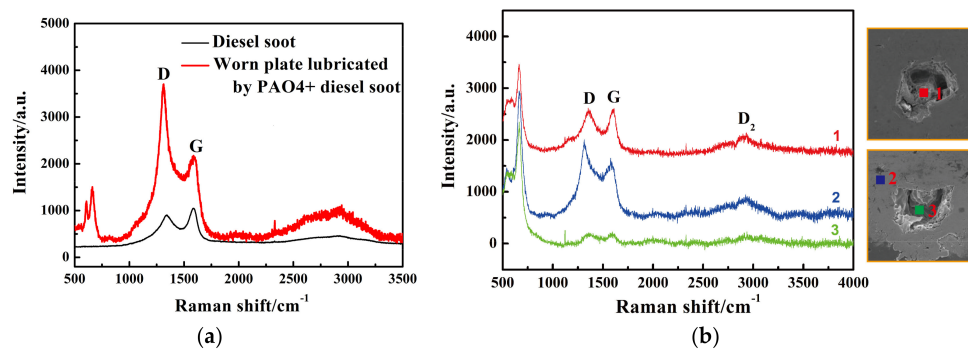
Figure 13. Raman spectra of the worn surfaces (*T* = 100 °C): (**a**) DS and the worn surface lubricated by oil + DS; (**b**) The peak in different worn position.
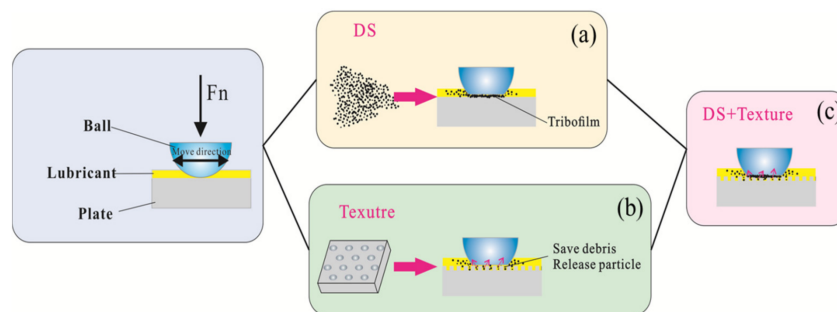

Figure 14. Schematic of the mechanism of the additive on the texture plate: (**a**) The function from DS; (**b**) The effect by texture; (**c**) The combined effect by DS and texture.
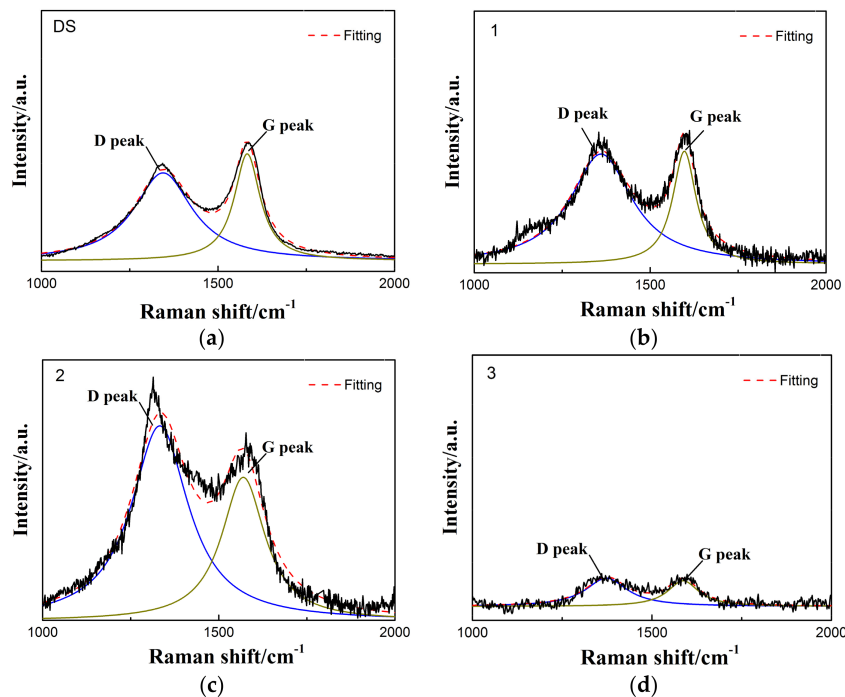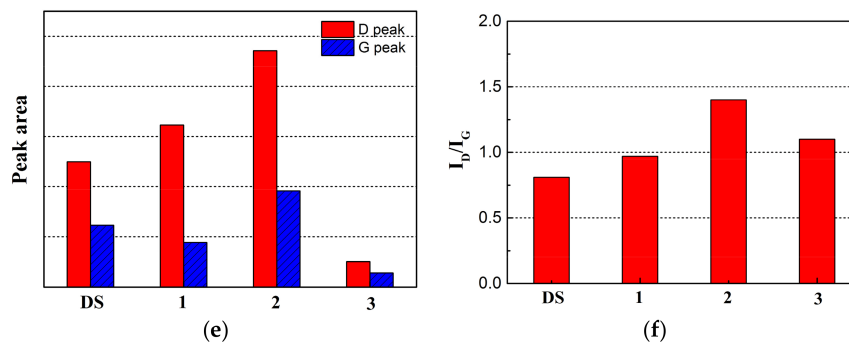

Figure 15. *Cont*.

Figure 15. Raman analysis. (**a**–**d**) Gaussian fitting applied for D and G peaks fitting of DS and 1#–3#. (**e**) The fitting results of the D and G peaks intensity, and (**f**) the intensity ratio of the D peak to the G peak (I_D/I_G).

4. Conclusions

A DS particle was used as an oil lubricating additive to investigate tribological behavior, and the combined effect of the DS particle with micro-texture was also studied. Through complete testing and analysis, the following conclusions can be drawn:

DS possesses a spherical structure, with a size ranging from 30 to 50 nm.

Higher friction coefficients from room temperature to 175 °C are obtained by laser surface texturing of spring steel with densities of 22.1% and 44.2%.

The textured surface, with a density of 44.2%, presents the lowest wear rate, and the composite effect of micro-texture and additive presents the optimal tribological performance.

The micro-dimple could promote the formation of the tribo-film and the storage function of the additive and wear debris, thereby enhancing the anti-wear property.

Author Contributions: Ming-Xue Shen and Zhen-Bing Cai conceived and designed the experiments; Jin-Fang Peng performed the experiments; Zhen-Bing Cai and Jin-Fang Peng analyzed the data; Ming-Xue Shen and Zhen-Bing Cai contributed reagents/materials/analysis tools; Jin-Fang Peng and Zhen-Bing Cai wrote the paper.

Conflicts of Interest: The authors declare no conflict of interest.

References

1. Reijnders, L. Human health hazards of persistent inorganic and carbon nanoparticles. *J. Mater. Sci.* **2012**, *47*, 5061–5073. [CrossRef]
2. Hamilton, D.; Walowit, J.; Allen, C. A theory of lubrication by micro-irregularities. *J. Basic Eng.* **1966**, *88*, 177–185. [CrossRef]
3. Nakano, M.; Korenaga, A.; Korenaga, A.; Miyake, K.; Murakami, T.; Ando, Y.; Usami, H.; Sasaki, S. Applying micro-texture to cast iron surfaces to reduce the friction coefficient under lubricated conditions. *Tribol. Lett.* **2007**, *28*, 131–137. [CrossRef]
4. Zhang, H.; Zhang, D.Y.; Hua, M.; Dong, G.N.; Chin, K.S. A Study on the tribological behavior of surface texturing on babbittalloy under mixed or starved lubrication. *Tribol. Lett.* **2014**, *56*, 305–315. [CrossRef]
5. Yu, H.W.; Wang, X.L.; Zhou, F. Geometric shape effects of surface texture on the generation of hydrodynamic pressure between conformal contacting surfaces. *Tribol. Lett.* **2010**, *37*, 123–130. [CrossRef]
6. Li, Y.Q.; Wang, T.M.; Pan, G.Q. Preparation and tribological properties of graphene oxide/nitrile rubber nanocomposites. *J. Mater. Sci.* **2012**, *47*, 730–738. [CrossRef]
7. Etsion, I. Modeling of surface texturing in hydrodynamic lubrication. *Friction* **2013**, *1*, 195–209. [CrossRef]
8. Etsion, I.; Halperin, G.; Becker, E. The effect of various surface treatments on piston pin scuffing resistance. *Wear* **2006**, *261*, 785–791. [CrossRef]

9. Etsion, I. Improving Tribological performance of mechanical components by laser surface texturing. *Tribol. Lett.* **2004**, *17*, 733–737. [CrossRef]

10. Braun, D.; Greiner, C.; Schneider, J. Efficiency of laser surface texturing in the reduction of friction under mixed lubrication. *Tribol. Int.* **2014**, *77*, 142–147. [CrossRef]

11. Schneider, J.; Braun, D.; Greiner, C. Laser Textured surfaces for mixed lubrication: Influence of aspect ratio, textured area and dimple arrangement. *Lubricants* **2017**, *5*, 32. [CrossRef]

12. Podgornik, B.; Vilhena, L.M.; Sedlacek, M.; Rek, Z.; Zun, I. Effectiveness and design of surface texturing for different lubrication regimes. *Meccanica* **2012**, *47*, 1613–1622. [CrossRef]

13. Gachot, C.; Rosenkranz, A.; Hsu, S.M. A critical assessment of surface texturing for friction and wear improvement. *Wear* **2017**, *372–373*, 21–41. [CrossRef]

14. Rosenkranz, A.; Pangraz, J.C.; Gachot, C. Load-dependent run-in and wear behaviour of line-like surface patterns produced by direct laser interference patterning. *Wear* **2016**, *368–369*, 350–357. [CrossRef]

15. Rosenkranz, A.; Szurdak, A.; Gachot, C. Friction reduction under mixed and full film EHL induced by hot micro-coined surface patterns. *Tribol. Int.* **2016**, *95*, 290–297. [CrossRef]

16. Ma, G.J.; Wang, L.L.; Gao, H.X.; Zhang, J.; Reddyhoff, T. The friction coefficient evolution of a TiN coated contact during sliding wear. *Appl. Surf. Sci.* **2015**, *345*, 109–115. [CrossRef]

17. Cai, Z.B.; Harry, M.M.; Ma, C.; Chi, M.F.; Luo, H.M.; Qu, J. Comparison of tribological behavior of steel-steel and Si_3N_4-steel contacts in lubricants containing ZDDP or ionic liquid. *Wear* **2014**, *319*, 172–183. [CrossRef]

18. Hu, E.Z.; Hu, X.G.; Liu, T.X.; Song, R.H.; Chen, Y.Z. Investigation of morphology, structure and composition of biomass-oil soot particles. *Appl. Surf. Sci.* **2013**, *270*, 596–603. [CrossRef]

19. Bhowmick, H.; Majumdar, S.K.; Biswas, S.K. Influence of physical structure and chemistry of diesel soot suspended in hexadecane on lubrication of steel-on-steel contact. *Wear* **2013**, *300*, 180–188. [CrossRef]

20. Joly-Pottuz, L.; Vacher, B.; Ohmae, N.; Martin, J.M.; Epicier, T. Anti-wear and friction reducing mechanisms of carbon nano-onions as lubricant additives. *Tribol. Lett.* **2008**, *30*, 69–80. [CrossRef]

21. Kinoshita, H.; Nishina, Y.; Alias, A.A.; Fujii, M. Tribological properties of monolayer graphene oxide sheets as water-based lubricant additives. *Carbon* **2014**, *66*, 720–723. [CrossRef]

22. Zin, V.; Agresti, F.; Barison, S.; Colla, L.; Mercadelli, E. Tribological properties of engine oil with carbon nano-horns as nano-additives. *Tribol. Lett.* **2014**, *55*, 45–53. [CrossRef]

23. Zhang, Z.C.; Cai, Z.B.; Peng, J.F.; Zhu, M.H. Comparison of the tribology performance of nano-diesel soot and graphite particles as lubricant additives. *J. Phys. D Appl. Phys.* **2016**, *49*, 045304. [CrossRef]

24. Guo, M.F.; Cai, Z.B.; Zhang, Z.C.; Zhu, M.H. Characterization and lubrication performance of diesel soot nanoparticles as oil lubricant additives. *RSC Adv.* **2015**, *5*, 101965–101974. [CrossRef]

25. Cizaire, L.; Vacher, B.; Mogne, T.L. Mechanisms of ultra-low friction by hollow inorganic fullerene-like MoS_2, nanoparticles. *Surf. Coat. Technol.* **2002**, *160*, 282–287. [CrossRef]

26. Nan, F.; Xu, Y.; Xu, B.S.; Gao, F.; Wu, Y.X.; Tang, X.H. Effect of natural attapulgite powders as lubrication additive on the friction and wear performance of a steel tribo-pair. *Appl. Surf. Sci.* **2014**, *307*, 86–91. [CrossRef]

27. Vlǎdescu, S.C.; Olver, A.V.; Pegg, I.G.; Reddyhoff, T. Combined friction and wear reduction in a reciprocating contact through laser surface texturing. *Wear* **2016**, *358–359*, 51–61. [CrossRef]

28. Zhang, H.; Qin, L.G.; Hua, M.; Dong, G.N.; Chin, K.S. A tribological study of the petaloid surface texturing for Co–Cr–Mo alloy artificial joints. *Appl. Surf. Sci.* **2015**, *332*, 557–564. [CrossRef]

29. Casiraghi, C.; Ferrari, A.C.; Robertson, J. Raman spectroscopy of hydrogenated amorphous carbons. *Phys. Rev. B* **2005**, *72*, 085401. [CrossRef]

30. Cai, Z.B.; Zhao, L.; Zhang, X.; Yue, W.; Zhu, M.H. Combined effect of textured patterns and graphene flake additives on tribological behavior under boundary lubrication. *PLoS ONE* **2016**, *11*, e0152143. [CrossRef] [PubMed]